

# Continuity Plate Detailing for Steel Moment-Resisting Connections

JEROME F. HAJJAR, ROBERT J. DEXTER, SARA D. OJARD, YANQUN YE, and SEAN C. COTTON

The 1994 Northridge, California earthquake resulted in the fracture of complete-joint-penetration groove (CJP) welds connecting girder flanges to column flanges in steel moment-resisting connections in a number of steel frame structures ranging from one to 26 stories in height (FEMA, 2000a). These welds fractured due to a combination of reasons, including the weld material having low fracture toughness; the pre-Northridge connection geometry making the CJP welds more susceptible to high strain and stress conditions; and welding practices that resulted in inconsistent weld properties (FEMA, 2000a). As a result of these fractures, in the subsequent years there has been a tendency to be more conservative than necessary in the design and detailing of steel moment-resisting connections both in seismic and non-seismic zones within the United States. In particular, continuity plates and web doubler plates have often been specified when they are unnecessary and, when they are necessary, thicker plates have been specified than would be required according to the applicable specifications. In addition, the welds of the continuity plates to the column flanges have often been specified as being complete-joint-penetration groove welds, even though the use of more economical fillet welds may have sufficed.

The tendency to be more conservative than necessary with the design of column stiffeners (i.e., continuity plates and doubler plates) is understandable since they do have a significant effect on the stress and strain distribution in the connection and on connection performance for columns with thinner flanges or webs. For example,

Roeder (1997) observed that girder-to-column joints with moderately sized continuity plates, doubler plates, or both performed better in cyclic loading tests than joints without such reinforcement. Also, it has been observed from finite element analyses of these joints that there is a decrease in stress concentration in the girder flange-to-column flange welds at the mid-width location of the girder flange when continuity plates are used (Roeder, 1997; El-Tawil, Vidarsson, Mikesell, and Kunnath, 1999). Nevertheless, if column flanges are sufficiently thick, experimental evidence exists that continuity plates are not required to achieve sufficient performance (Ricles, Mao, Kaufmann, Lu, and Fisher, 2000; Lee, Cotton, Dexter, Hajjar, Ye, and Ojard, 2002).

The design criteria for the limit states applicable to continuity plate and doubler plate design for non-seismic conditions are provided in Section K1 of Chapter K of the American Institute of Steel Construction (AISC) *Load and Resistance Factor Design (LRFD) Specification for Structural Steel Buildings* (AISC, 1999a). There are additional, more stringent provisions in the requirements for Special Moment Frames (SMF) in the AISC *Seismic Provisions for Structural Steel Buildings* (AISC, 1992). However, the 1997 and 2002 AISC *Seismic Provisions* (AISC, 1997a, 2000, and 2002) removed all design procedures related to continuity plates, requiring instead that they be proportioned to match those provided in the tests used to qualify the connection.

As part of the SAC Joint Venture research program, preliminary post-Northridge seismic design guidelines and two advisories were published (FEMA, 1995; FEMA, 1996; FEMA, 1999) that pertained to these column reinforcements in seismic zones. For example, the guidelines called for continuity plates at least as thick as the girder flange that must be joined to the column flange in a way that fully develops the strength of the continuity plate, i.e. this encouraged the use of complete-joint-penetration groove (CJP) welds. However, more recent seismic guidelines (FEMA, 2000a) have reestablished design equations to determine whether continuity plates are required and, if so, what thickness is required.

Recent research has revealed that excessively thick continuity plates are unnecessary. El-Tawil and others (1999) performed parametric finite element analyses of girder-to-column joints. They found that continuity plates are

---

Jerome F. Hajjar is associate professor, department of civil engineering, University of Minnesota, MN.

Robert J. Dexter is associate professor, department of civil engineering, University of Minnesota, MN.

Sara D. Ojard is structural engineer, Geiger Engineers, Bellingham, WA.

Yanqun Ye is structural engineer, Thornton-Tomasetti Engineers, Chicago, IL.

Sean C. Cotton is structural engineer, Hammel Green and Abrahamson, Inc., Minneapolis, MN.

---

increasingly effective as the thickness increases to approximately 60 percent of the girder flange. However, continuity plates more than 60 percent of the girder flange thickness brought diminishing returns.

Furthermore, over-specification of column reinforcement may actually be detrimental to the performance of connections. As continuity plates were made thicker and attached with highly restrained CJP welds, they sometimes contributed to cracking during fabrication (Tide, 2000). Yee, Paterson, and Egan (1998) performed finite element analyses comparing fillet-welded and CJP-welded continuity plates including heat input of the weld passes. Based on principal stresses extracted at the weld terminations, it was concluded that fillet-welded continuity plates may be less susceptible to cracking during fabrication than if CJP welds are used.

The research described in this paper is part of an ongoing project to reassess the design provisions for column stiffening, including both continuity and doubler plate detailing, for non-seismic and seismic design conditions, and to investigate new alternative column stiffener details. The project includes three components: monotonically loaded pull-plate experiments to investigate the need for and behavior of continuity plates (Prochnow, Dexter, Hajjar, Ye, and Cotton, 2000), cyclically loaded cruciform girder-to-column joint experiments to investigate panel zone behavior and local flange bending (Lee and others, 2002), and parametric finite element analyses (FEM) to corroborate the experiments and assess the performance of various continuity plate and doubler plate details (Ye, Hajjar, Dexter, Prochnow, and Cotton, 2000; Webster, 2000). Throughout the project, new doubler plate and continuity plate details were investigated to explore economical detailing and minimize welding along the column *k*-line region, as per the recommendations of the AISC advisory for the *k*-line region (AISC, 1997b). New column stiffener details that were investigated included: continuity plates that were half the thickness of girder flange and that were fillet-welded to the column; doubler plates that were fillet-welded to the column flanges; and doubler plates that were offset from the column flanges by several inches to serve as both doubler and continuity plates. In addition, several unstiffened column specimens were analyzed and tested to verify where stiffeners are not required in steel connection design.

This paper presents the results of the pull-plate experiments and analyses, and the relation of these results to the AISC provisions for continuity plate design. These monotonic tests focus on non-seismic design provisions, although some consideration is given to seismic design as well. Because pull-plate specimens are loaded in monotonic tension, the primary focus of these tests was on continuity plate detailing. Lee and others (2002) discuss in more depth the related doubler plate detailing issues considered in this

research. The paper includes background on the primary limit states for continuity plate design, including local web yielding (LWY) and local flange bending (LFB), as well as a presentation of historical conclusions from previous research regarding the behavior of continuity plates and the welds attaching them to the columns. Also, included is a brief description of the finite element analysis models that were used in this research to further understand the behavior of the tested specimens and to corroborate with the experimental tests. The results of the pull-plate specimens are then presented and compared to defined failure modes and yield mechanisms relating to the limit states of LWY and LFB. The paper concludes by comparing the results to current AISC design provisions, discussing the behavior of the new column detailing, and presenting proposed new design equations for the LWY and LFB limit states.

## BACKGROUND

The present AISC (1999a) non-seismic provisions that govern the design of continuity plates are based on three limit states: local web yielding (LWY), local flange bending (LFB), and local web crippling (LWC). An overview of the developments of the provisions for local web yielding and local flange bending is presented in this section. However, web crippling is not discussed, as it rarely controls continuity plate design (Dexter, Hajjar, Cotton, Prochnow, and Ye, 1999; Prochnow and others, 2000).

A provision to restrict LWY of column sections was first defined in the 1937 AISC Manual (AISC, 1937). The provision remained the same until after the research of Sherbourne and Jensen (1957) and Graham, Sherbourne, Khabbaz, and Jensen (1960), which was focused on investigating column web and flange behavior in moment-resisting frame connections and updating design specifications related to stiffener connection design. The outcome of the research generated guidelines for the use and sizing of continuity plates, which were first used in various forms in the AISC Allowable Stress Design (ASD) Specifications (e.g., AISC, 1989). This equation, as shown below, is still used in the current AISC LRFD non-seismic provisions for the limit state of local web yielding (AISC, 1999a).

$$R_u < \phi R_n = \phi(5k + N)F_{yc}t_{cw} \text{ for interior conditions} \quad (1)$$

$$R_u < \phi R_n = \phi(2.5k + N)F_{yc}t_{cw} \text{ for end conditions} \quad (2)$$

where:

$$\phi = 1.0$$

$$R_u = \text{required strength}$$

$$R_n = \text{nominal strength}$$

$$k = \text{distance from outer face of flange to web toe of fillet}$$

$N$  = length of bearing surface (typically taken as the thickness of the girder flange)  
 $F_{yc}$  = minimum specified yield strength of the column  
 $t_{cw}$  = thickness of column web

The current non-seismic design equation for LFB is also based on the research work of Graham and others (1960), in conjunction with limit load and buckling analyses of Parkes (1952) and Wood (1955). The equation is a result of using plastic yield line analysis to fit the experimental results regarding local flange bending of the tests and lower bound approximations of dimensions of common girder and column combinations of the time. A modified form of the LFB equation from Graham and others (1960) is currently used in the LRFD Specification (AISC, 1999a), which requires that the design strength of the column flanges exceed the concentrated transverse force applied by the girder flange across the column flange. The design strength of the column flange for the local flange bending limit state is given as:

$$\phi R_n = \phi 6.25 t_{cf}^2 F_{yc} \quad (3)$$

where:

$\phi = 0.9$   
 $t_{cf}$  = thickness of the column flange

Since the research of Graham and others (1960), several researchers have examined the behavior of moment-resisting connections with and without continuity plates, and have recommended various methods of sizing continuity plates. Since the 1994 Northridge earthquake, the trend in continuity plate design for seismic moment frames has been to require stiffeners sized to have a thickness equal or larger than the thickness of the larger girder flange framing into the connection, regardless of the required strength. Furthermore, continuity plates were often previously fillet-welded to the column web and flanges. After the Northridge earthquake, it has been typical to use CJP welds to join the continuity plates to the column flanges, and often to the web as well.

The following is a summary of significant past conclusions from researchers regarding continuity plate design:

- Johnson performed three different series of tests (Johnson, 1959a, 1959b, 1959c) on a total of 31 fully-welded connections with and without continuity plates and 22 pull-plate tests, all subjected to monotonic loading. The final conclusions of the tests were that continuity plates should be half the width of the girder flange and approximately the same thickness, and that fillet welds were sufficient to connect the stiffeners to the column flanges.
- Popov, Amin, Louie, and Stephen (1986) performed a series of cyclic half-scale cruciform tests, with and without continuity plates, to verify the design criteria for girder-to-column connections in seismic conditions. The results of the tests showed that, for two connections consisting of the same column and girder sizes, the inelastic girder rotation greatly increased when continuity plates were included in the connection. Yielding and buckling of the continuity plates was witnessed when the girders were within the strain-hardening range. Thus, the researchers concluded that designing stiffeners on the basis of nominal yielding in the girder flanges was unconservative. Regarding the continuity plate welds, recommendations were made to use complete-joint-penetration groove welds to attach the continuity plates to the column flanges, rather than fillet welds, since a fillet weld connecting the continuity plate to the column flange failed prematurely in one of the two connections using fillet welds all around the continuity plates.
- Tremblay, Timler, Bruneau, and Filiatrault (1995) outlined the characteristics of the AISC seismic design provisions (AISC, 1992), summarized reconnaissance site visits of several buildings after the Northridge earthquake, and compared the observed behavior to the expected performance. From observations of actual performance, the authors contended that the presence of continuity plates may have played a role in mitigating weld failures. The connections with continuity plates had fewer weld failures, which suggested that the flexibility of the column flanges could have resulted in local overstressing of the welds. Tremblay and others (1995) recommended the use of continuity plates in all connections designed for seismic zones.
- Kaufmann, Xue, Lu, and Fisher (1996) and Xue, Kaufmann, Lu, and Fisher (1996) tested several fully welded girder-to-column connections under cyclic loading. The connections varied the type of welding electrodes used in the girder-to-column CJP weld. Each of the connections contained continuity plates joined to the column flanges and webs with  $\frac{5}{8}$ -in. fillet welds. The results of the tests showed that fully welded connections that used electrodes with higher toughness values and fillet-welded continuity plates can act in a ductile manner.
- Roeder (1997) performed finite element analyses for critical components of pre-Northridge connections. These localized analyses showed that transverse strains in the girder and column flange are restrained by the surrounding steel, and are therefore susceptible to hydrostatic tensile stress and potential cracking. The author also showed that continuity plates may decrease the hydrostatic stress at the girder-to-column interface,

which then may affect the likelihood of weld cracking. Roeder (1997) gave no recommendations on the most effective size of continuity plates in moment-resisting frames.

- Engelhardt, Shuey, and Sabol (1997) tested three welded flange-bolted web moment connections under cyclic load to failure. The connections were then repaired and retested. The test results showed that repairing connections by using high toughness weld metal makes the connection behave adequately under cyclic loads. The authors recommended using CJP welds to attach the continuity plates to the column flanges and fillet welds to attach to the column web.
- Welding of the continuity plates to the column flanges potentially creates a highly restrained configuration and generates large tensile residual stresses. Since it became customary to use CJP welds and thicker continuity plates, a number of fractures of the k-line region of the column web were occurring during fabrication (Tide, 2000). The AISC advisory for the k-line region (AISC, 1997b) recommended that the welds for continuity plates should stop before the k-line. The AISC advisory (AISC, 1997b) also recommended that all continuity plate welds should be fillet welds or partial-joint-penetration groove welds.
- Yee and others (1998) performed finite-element simulations, including heat input of weld passes, on connections with continuity plates, which were attached by CJP welds or fillet welds. The analyses resulted in higher residual stresses occurring when the stiffeners were attached with CJP groove welds. This led to the recommendation that fillet welds should be used to avoid brittle fracture.
- El-Tawil and others (1999) performed finite element analyses on a cantilever connection, with various continuity plate thicknesses ranging from half of the girder flange thickness to full-thickness. The analyses concluded that continuity plates with thicknesses less than 60 percent of the girder flange thickness resulted in very similar stress and strain distributions compared to the results of those with continuity plates as thick as the girder flanges.
- Dexter and Melendrez (2000) tested over 40 pull-plate tests with 100 ksi yield strength pull plates to investigate the through-thickness strength of the column flanges. Most of the specimens had fillet-welded continuity plates. These fillet-welded continuity plates performed adequately provided they were detailed in accordance with the AISC advisory (AISC, 1997b).

- Bjorhovde and others (1999) tested a series of cyclically-loaded one-sided cruciform tests with relatively weak panel zones. These specimens had fillet-welded continuity plates that met criteria of the AISC k-line advisory (AISC, 1997b). The continuity plates and connections performed adequately.
- Engelhardt (1999) made preliminary recommendations for the design and detailing of reduced beam section (RBS) moment connections based on available experimental data on the connections. Recommendations were made to use continuity plates with thicknesses similar to the beam flange thickness in all RBS connections, which were CJP-welded to the column flanges and webs. However, none of the RBS tests omitted continuity plates, so it is unclear what conditions should require continuity plates.
- Ricles and others (2000) tested four cruciform specimens, with and without continuity plates. The continuity plates were attached to the column flanges with CJP welds. The tests showed that continuity plates improve performance of the connections, but that satisfactory behavior can be achieved if the column flanges are sufficiently thick. An additional equation, similar to that discussed below in relation to FEMA (2000a), was proposed that defined the required continuity plate thickness in terms of the girder flange width.
- Roeder discussed the results of the research conducted by the SAC Joint Venture in FEMA (2000d). The continuity plate requirements presented were essentially the same equations as the AISC Seismic Provisions (AISC, 1992), such that continuity plates were required if:

$$t_{cf} < 0.4 \sqrt{\frac{R_u}{F_{yc}}} \quad (4)$$

where:

$$R_u = 1.8F_{yg}A_{gf} \quad (5)$$

$$A_{gf} = b_{gf}t_{gf}$$

$b_{gf}$  = width of the girder flange

$t_{gf}$  = thickness of the girder flange

The 1.8 factor in the equation for the seismic girder demand  $R_u$  includes a strain hardening factor of 1.3 on the yield strength, and assumes the full plastic capacity of the girder is carried by the flanges. Thus, the 1.3 factor is increased by the ratio of the plastic section modulus,  $Z_x$ , to the flange plastic section modulus,  $Z_f$  of the girder. This ratio is typically at most approximately 1.4 for rolled wide-flange shapes, resulting in the factor of 1.8 ( $1.4 \cdot 1.3 \approx 1.8$ ) (Bruneau, Uang, and Whittaker, 1998).

**Table 1. Nominal Dimensions and Normalized Design Strengths of Candidate Pull-Plate Specimens (Unstiffened)**

Nominal Dim.	Column	W14x120	W14x132	W14x145	W14x159	W14x176
	$t_{cw}$	0.590	0.645	0.680	0.745	0.830
	$t_{cf}$	0.940	1.030	1.090	1.190	1.310
	$k$	1.625	1.688	1.750	1.875	2.000
Non-seismic*	LWY	0.70	0.79	0.86	1.01	1.19
	LFB	0.66	0.80	0.89	1.06	1.29
$1.1R_y^*$	LWY	0.58	0.66	0.72	0.84	0.99
	LFB	0.55	0.66	0.74	0.89	1.07
Seismic*	LWY	0.39	0.44	0.48	0.56	0.66
	LFB	0.37	0.44	0.50	0.59	0.72

\* The values in the table are the ratio of  $\phi R_n/R_u$ , which show the percentage of the flange force the column can resist. Equations (8), (9), and (5) were used to determine  $R_u$  based on non-seismic,  $1.1R_y$ , and seismic girder flange demands, respectively, while Equations (1) and (3) were used to calculate  $\phi R_n$  for LWY and LFB, respectively.

An additional equation presented in the research by Ricles and others (2000) and similar to Equation 7 below was also included in FEMA (2000d) as a possible addition to the continuity plate requirements. Because the tests of Ricles and others (2000) showed that Equations 4 and 5 provided a conservative measure of the continuity plate requirements, Roeder concluded that it was appropriate to return to the requirements of the 1992 Seismic Provisions (AISC, 1992).

- FEMA (2000a), resulting from the research of the SAC Joint Venture, uses the LFB equation and a seismic girder demand to calculate the need for continuity plates. The guidelines state that unless proven with tested connections, continuity plates are required if the thickness of the column flange is less than either of the two following equations:

$$t_{cf} < 0.4 \sqrt{1.8 b_{gf} t_{gf} \left( \frac{F_{yg}}{F_{yc}} \right)} \quad (6)$$

$$t_{cf} < \frac{b_{gf}}{6} \quad (7)$$

In summary, there is some consensus that continuity plates may be fillet-welded and may not always be required in non-seismic connections. However, there is a prevailing consensus that continuity plates are generally required for

connections in seismic zones, although there are differing conclusions on the required width and thickness of the plate, on the type of weld that should be used to connect the stiffener to the column flange, and on whether very thick column flanges always require continuity plates.

### SPECIMEN SELECTION

A substantial parametric study was conducted (Prochnow and others, 2000) to assess appropriate girder and column combinations for the pull plate tests. Parameters were studied that affected continuity plate requirements for columns designed either for non-seismic or seismic detailing conditions. From this study, a range of column sections were identified as being on the cusp of the LWY and LFB limit states, as defined by Equations 1 and 3, respectively, and using required strengths,  $R_u$ , based upon non-seismic and seismic girder flange demands, which were calculated as:

$$R_u = 1.0 F_{yg} A_{gf} \quad (\text{non-seismic girder flange demand}) \quad (8)$$

$$R_u = 1.1 R_y F_{yg} A_{gf} \quad (\text{seismic girder flange demand}) \quad (9)$$

where:

$$R_y = \begin{aligned} &\text{ratio of expected yield strength to minimum specified yield strength} \\ &= 1.1 \text{ for grade 50 or 65 rolled shapes.} \end{aligned}$$

Equation 8 is typically used for non-seismic design, representing the nominal yield strength of the flange. Equation 5, representing one alternative value for seismic girder flange demand, predicts stresses in the flange well above the tensile strength of most structural steels. Equation 9, presented by Prochnow and others (2000), provides a more realistic flange force for use in assessing the results of the pull-plate experiments. The  $1.1R_y$  factor is consistent with the strong column-weak beam check and panel zone demand calculations used by AISC (1997a, 1999b, 2002).

Five W14 sections in particular were isolated for further investigation, including W14×120, W14×132, W14×145, W14×159, and W14×176 columns. These were coupled with a pull plate representing a W27×94 girder flange. Using the girder nominal yield strength of 50 ksi and girder flange (i.e., pull-plate) dimensions, the girder flange demands were approximately 375 and 450 kips from Equations 8 and 9, respectively. Table 1 summarizes the ratios of the design strength to required strength for the limit states of LWY and LFB using the three different girder flange demands from Equations 5, 8, and 9 and, for the design

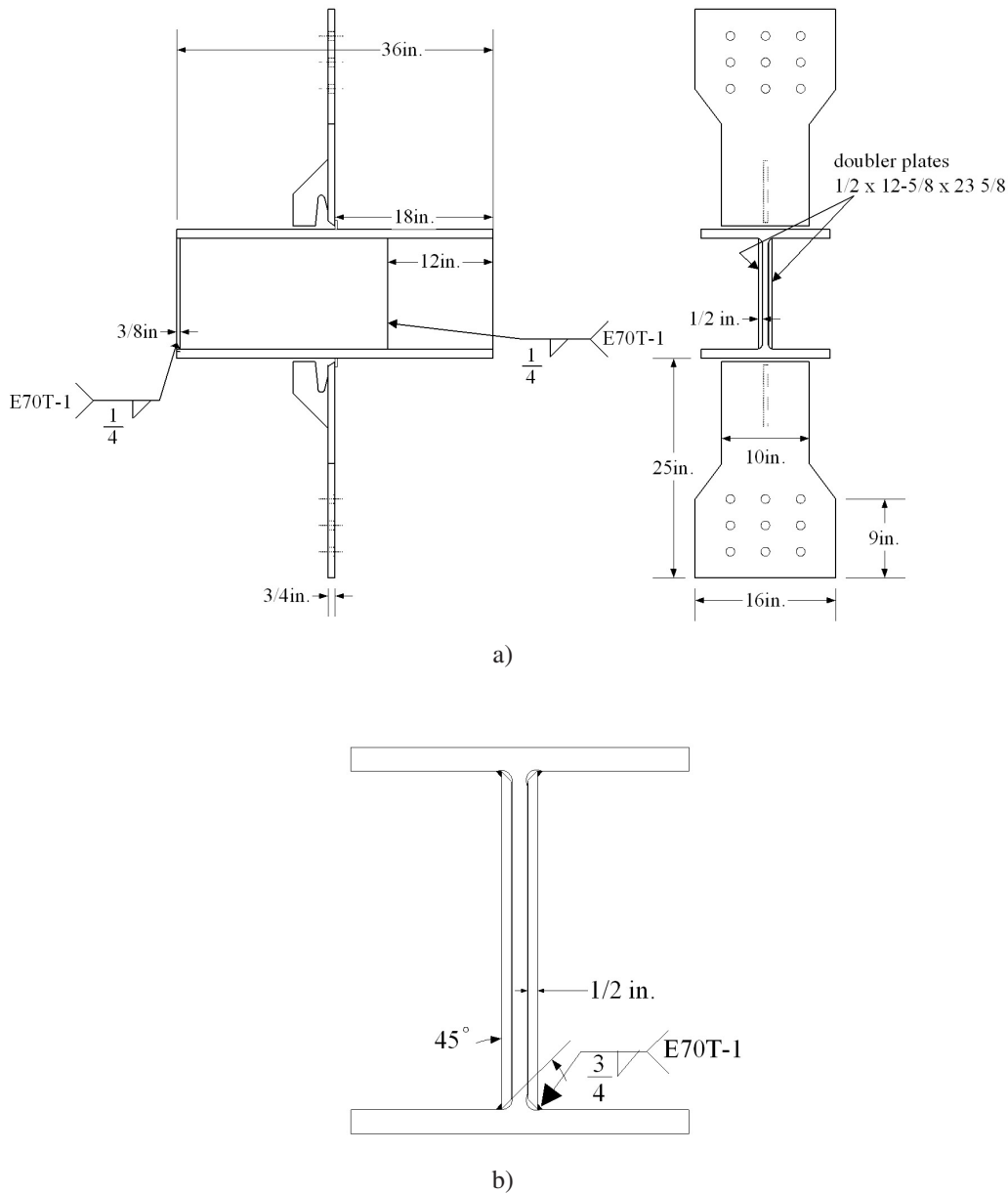


Fig. 1. Typical pull-plate specimen with beveled, fillet-welded doubler plate.

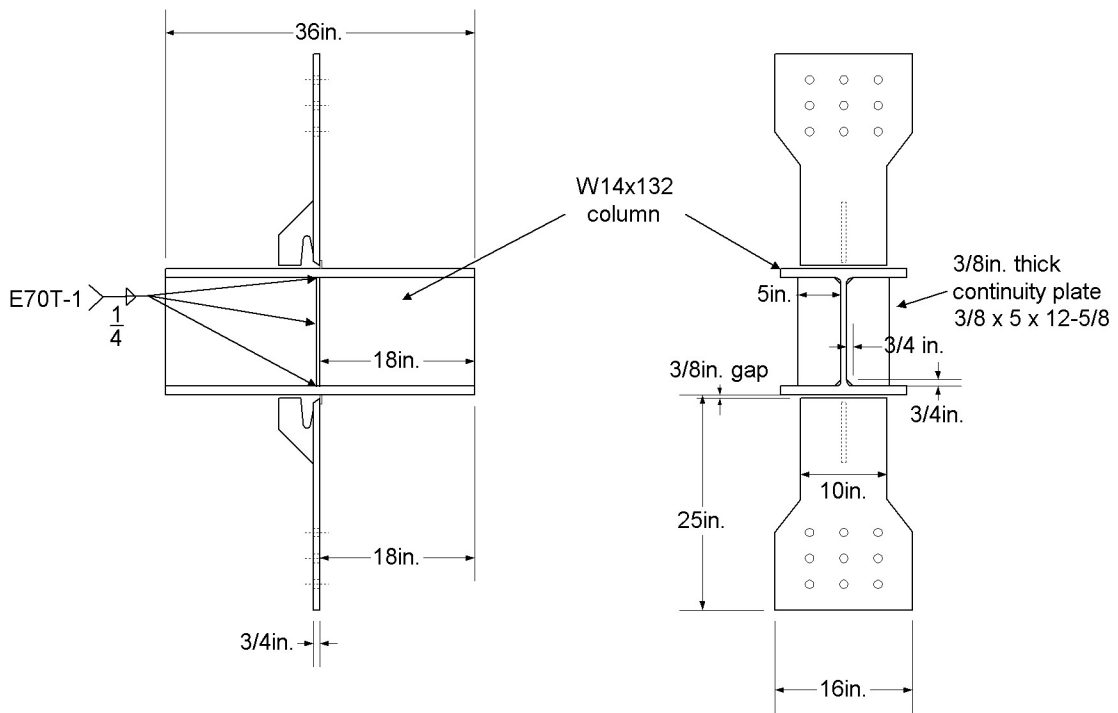


Fig. 2. Typical pull-plate specimen with a half-thickness continuity plate, fillet-welded to the column flange and web.

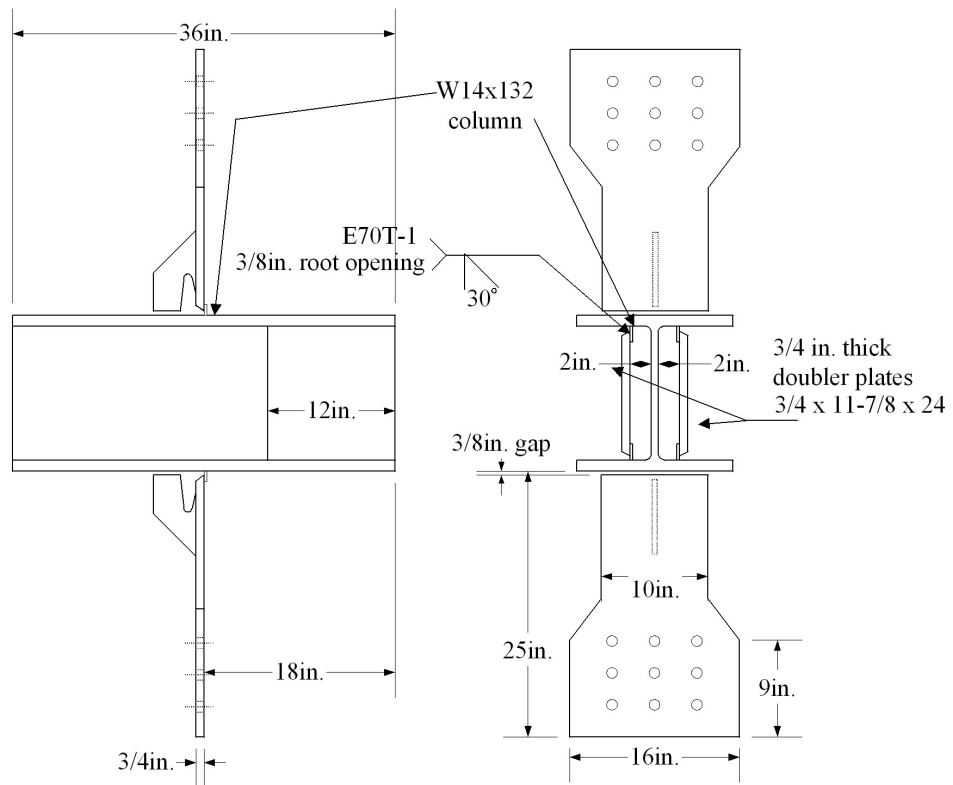


Fig. 3. Typical pull-plate specimen with a box detail consisting of doubler plates welded to the column flange away from web with CJP welds.

strengths, nominal dimensions from AISC (1995) as shown in the table and a column nominal yield strength of 50 ksi. Note that AISC (1995) did not distinguish between design and detailing  $k$ -dimensions, but the values from AISC (1995) are close to the corresponding new design  $k$ -dimensions discussed in AISC (2001).

Finite element models of the proposed pull-plate test setup were then analyzed and compared for these five column sizes to help finalize the specimen selection. The finite element analyses were used to help determine the appropriate specimen sizes, to select the appropriate length of the column stub, and to define failure criteria for the LWY and LFB limit states. Details of the finite element models are given in Ye and others (2000).

Figures 1 through 4 show the details of the pull-plate specimens used in this research (Prochnow and others, 2000). The pull-plate specimens consisted of three-foot-long sections of columns with pull plates welded to the column flanges, representing the flanges of the girders in the actual connections. Actual nominal dimensions of a W27×94 flange are  $t_{gf} = 0.745$  in. and  $b_{gf} = 9.995$  in. The pull-plates were constructed as  $\frac{3}{4}$  in. by 10 in. plates. Based on the use of a W27×94 girder and column sections all made from A992 steel, none of the girder-to-column combinations satisfy the strong column-weak beam criteria from AISC (1997a, 2000, 2002), as the overriding objective was to impart a large flange force onto a relatively weak column section so as to test the extreme limits of the associated limit states.

For the finite element analyses, the columns were modeled using nominal section dimensions. One-quarter of each specimen was used in the finite element model. All of these finite element models used for specimen design consisted of unstiffened sections and pull-plates representing a W27×94 girder flange. The unstiffened pull-plate model typically consisted of approximately 4725 nodes and 3275 elements. Generally, the mesh consisted of four layers of elements through the thickness of the pull plate, the column web, and the continuity plate; three layers of elements through the column flange thickness; 17 elements along the half width of the column flange; and 11 elements along the half depth of the column web. However, at areas of high stress concentrations, such as directly below the pull-plate in the column  $k$ -line, smaller elements were used to more accurately define the behavior of the specimens. A mesh refinement study was conducted on an unstiffened specimen with a 2 ft column stub length, refining the mesh everywhere where high stress and strain gradients were observed. The results of the study indicated the coarser mesh to be sufficient for the analysis [details can be found in (Ye and others, 2000)].

The models were constructed using A992 column sections and A572 Gr. 50 plate material for the pull-plates. For the preliminary finite element analyses, the nominal minimum specified yield strength,  $F_{yn}$ , of 50 ksi was used for all column sections and plate material. The input data for the finite element models were simplified piecewise linear stress-strain curves based on the results of tensile tests conducted by Frank on a sampling of currently rolled shapes

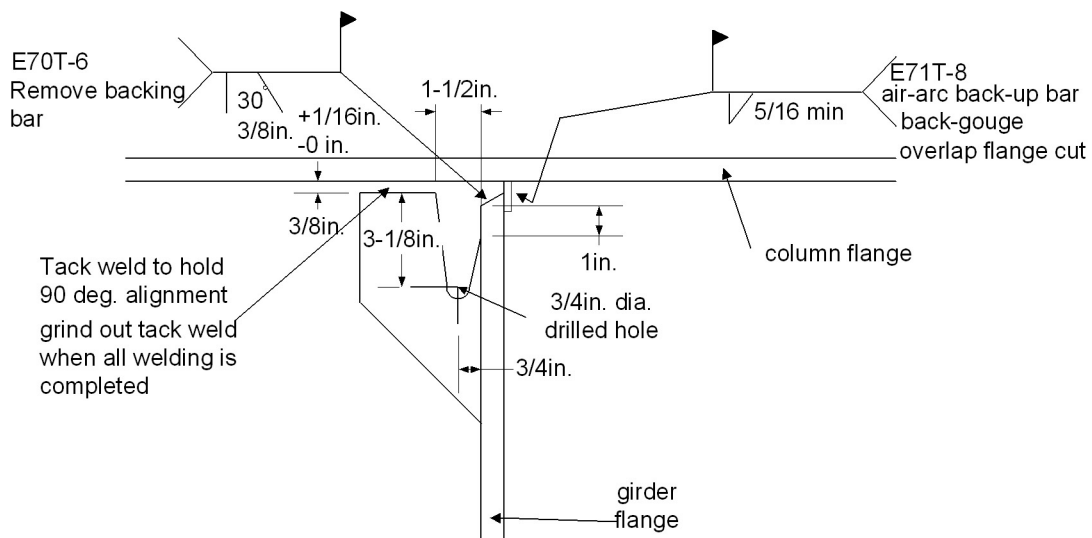


Fig. 4. Typical pull plate-to-column weld detail.

(FEMA, 2000b). Figure 5 shows this stress-strain curve, based on Frank's research, for the A992 steel used in the preliminary finite element models. The curve was defined by the nominal yield strength  $F_{yn}$  and by the nominal yield strain  $\epsilon_{yn} = F_{yn} / E$ , where  $E$  is Young's modulus, which was taken as 29,000 ksi.

The stress-strain curve of the weld metal was selected to be similar to that of the base metal, except that a shorter yield plateau and more gradual strain-hardening progression were used. A yield strength of 75 ksi and a tensile strength of 80 ksi was used in the finite element models [these values are within the range of properties provided by the catalog of the vendor that supplied the weld metal used for this research; details can be found in (Ye and others, 2000)].

The finite element models were compared, including key comparisons at five different locations: one measurement of flange displacement and strain measurements at two locations each in the column flanges and column webs. A sample of the results is shown in Figures 6 through 8. Figure 6 shows a typical deformed shape at 5 percent total elongation of the W14x132 pull-plate specimen from tip-to-tip of the pull-plates, showing the complex three-dimensional displacement pattern exhibited by local flange bending failure coupled with local web yielding. For Figures 7 and 8, the comparisons are reported at a load of approximately 400 kips for four out of five of the column sections studied. This load level was chosen since it is greater than the nominal yield strength of the pull-plates of 375 kips, calculated by Equation 8, and is also greater than the loads that the columns can resist for either LWY or LFB, calculated by Equations 1 and 3.

As can be seen in Figures 7 and 8, there is a considerably larger change in strain and displacement between the W14x120 and W14x132 column sections than when comparing the other sections. Figure 7 shows that the W14x120 had a strain along the k-line of 4 percent at a distance of  $(5k+N)/2$  from the column centerline (i.e., the line traced parallel to the line of force,  $P_{uf}$ , and located where the pull plates intersect the column, as shown in Figure 7), as well as 40 percent strain along the k-line at the centerline of the column length; these are excessive values, thus clearly indicating this column would have exceeded the LWY limit state. The same figure shows that the W14x132 exhibited much more reasonable behavior, but still would likely fail by LWY. The strain at a distance of  $(5k + N)/2$  was predicted as 0.18 percent (approximately equal to the yield strain), and at the centerline the value was 10 percent, as seen in Figure 7. Figure 8 also shows that the W14x120 exhibited excessive flange tip deflection due to local flange bending (combined with local web yielding). The W14x132 also had a large flange tip deflection compared to the larger sections. According to the AISC LRFD Specification (AISC, 1999a), all of the lightest three sections, including the W14x145, would need continuity plates for both the LWY and LFB limit states for non-seismic applications (see Table 1). Therefore, since both the W14x132 and W14x145 needed stiffeners according to the specification, and the finite element analyses predicted a reasonable possibility of LWY and LFB failure for the W14x132 but lower likelihood of reaching the limit states for non-seismic demand for the W14x145, the W14x132 was chosen as the smallest section to test the LWY and LFB limit states. A W14x159 section was also tested unstiffened to ensure testing of a column that exhibited little possibility toward fail-

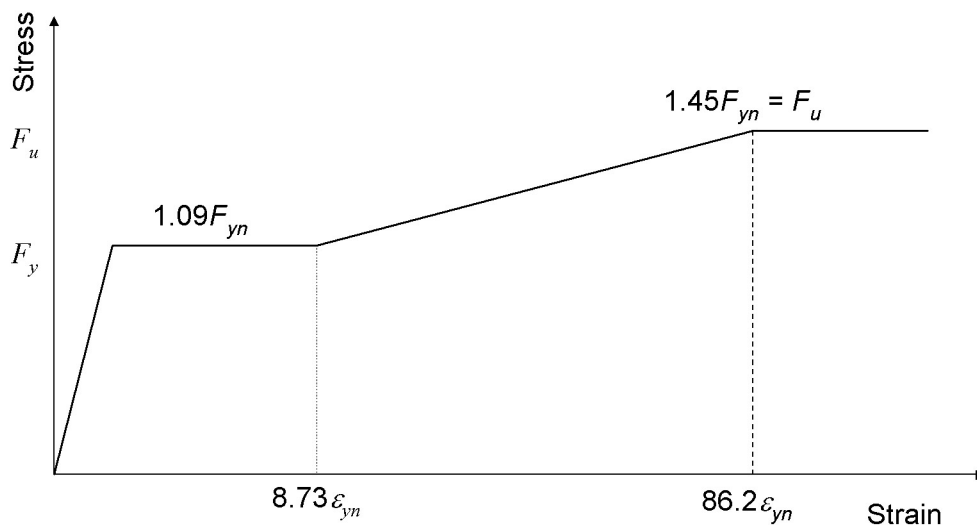


Fig. 5. Stress-strain curve of A992 steel used for preliminary finite element analyses of pull-plate specimens.

ure. In addition, a W14×132 and a W14×159 were tested with doubler plates to mitigate LWY, so as to focus on the distinction in the LFB response of these specimens. Four stiffened W14×132 specimens, described more in the next section, completed the test matrix.

### SPECIMEN DESIGN

Nine pull-plate specimens were tested in this research, using the three column sections outlined in the prior section, as follows:

1. Specimen 1-LFB: W14×132 without continuity plates, with doubler plates, examined LFB
2. Specimen 2-LFB: W14×145 without continuity plates, with doubler plates, examined LFB
3. Specimen 1-LWY: W14×132 without any continuity or doubler plates, examined LWY and LFB
4. Specimen 2-LWY: W14×145 without any continuity or doubler plates, examined LWY and LFB
5. Specimen 3-UNST: W14×159, without any continuity or doubler plates, examined LWY and LFB
6. Specimen 1-FCP: W14×132, with full-thickness continuity plates and CJP welds
7. Specimen 1-HCP: W14×132, with half-thickness continuity plates and fillet welds
8. Specimen 1B-HCP: repeat of 1-HCP to verify results
9. Specimen 1-DP: W14×132, with doubler plate box detail

The nine specimens may be grouped into three categories (with some specimens contributing to more than one category): specimens focused on evaluating the LFB limit state, specimens used to evaluate the LWY limit state (and the interaction of LWY and LFB), and specimens aimed at investigating the effects of new stiffening details on the connections. The specimens all included a pull-plate whose dimensions are approximately equal to the nominal dimensions of the girder flange of a W27×94. This girder section was chosen because it is commonly used today and because it places a high flange force demand on the columns. To ensure consistency in the demand placed on the columns, the girder flange area was not a variable in this study.

Specimens 1 and 2 included a new doubler plate detail in which beveled doubler plates were fillet-welded to the column flange to avoid welding in the column *k*-line (see Figure 1). The doubler plates stiffened the web of the two specimens in order to isolate local flange bending as the governing limit state. The fillet weld sizes were chosen to satisfy both the strength requirement (i.e., full development of the doubler plate in shear) and geometric requirements as outlined in AISC (1999b). Specimens 3 through 5 were unstiffened connections that looked at the interaction between LWY and LFB. Specimens 6 through 8 tested connections either with full-thickness continuity plates and CJP welds, replicating details often seen in current practice, or half-thickness continuity plates with fillet welds; Specimen 8 repeats the experiment of Specimen 7 to help verify the results of this economical continuity plate detail (see Figure 2). The continuity plates all had 3/4-in. clips, and for Specimens 7 and 8, the fillet weld along the web was terminated an additional 3/4-in. from the toe of the clip to help mitigate stress concentrations near the column *k*-line. Specimen 9 included no continuity plate, but rather two doubler plates placed out

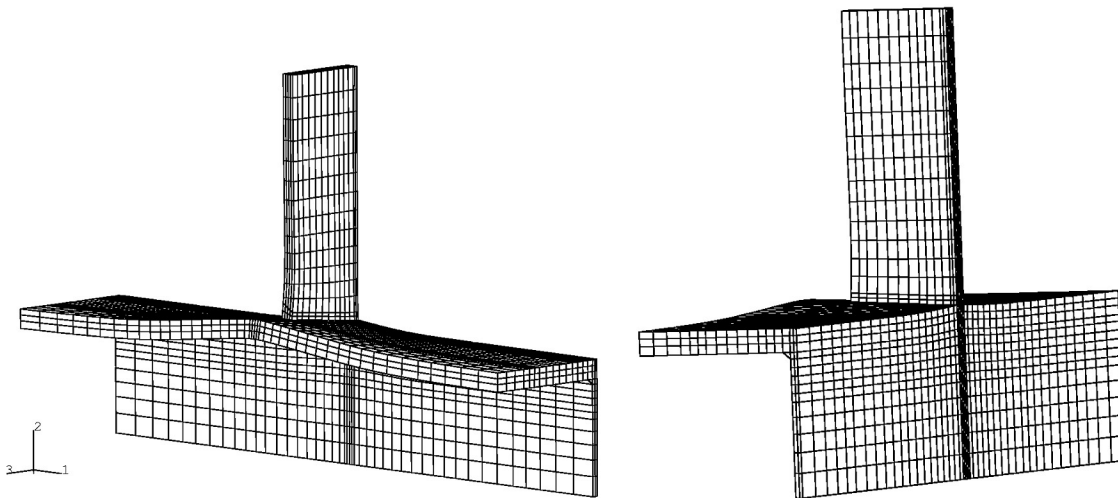
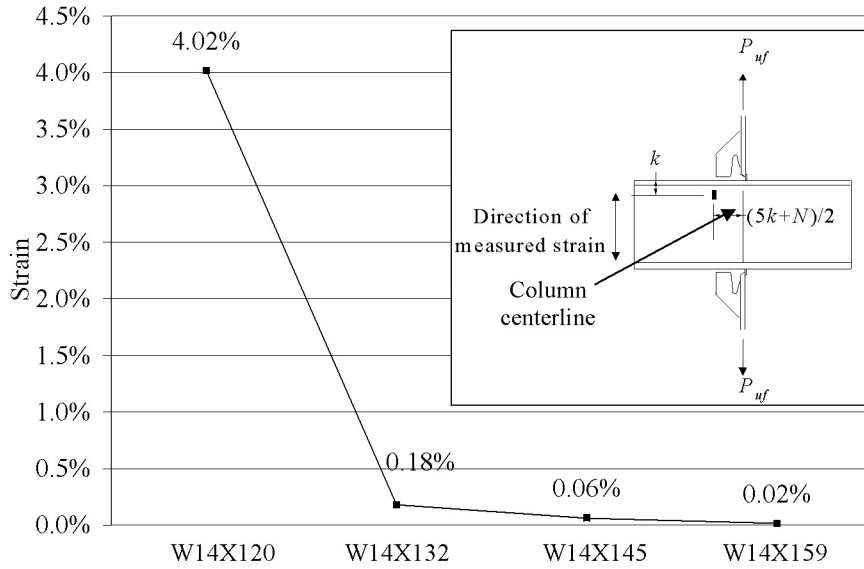


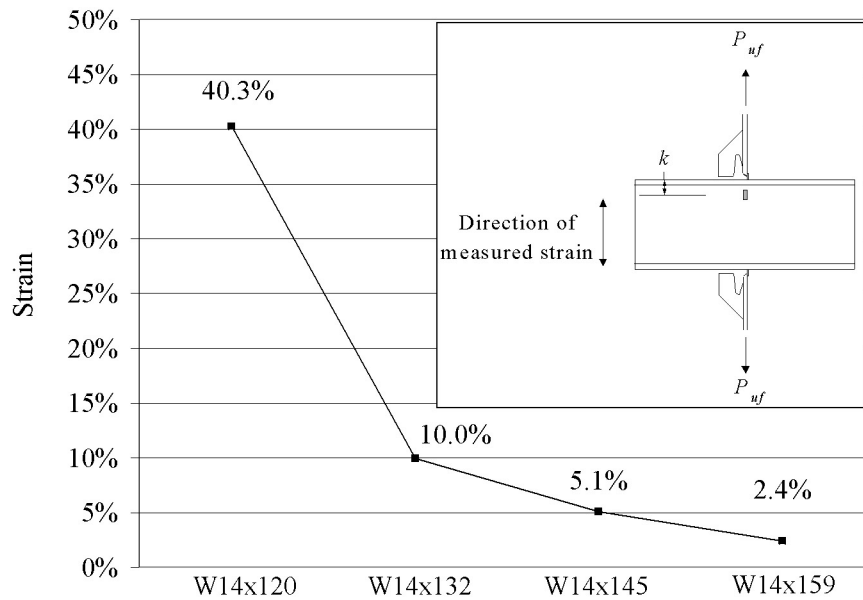
Fig. 6. Deformed shape for unstiffened W14×132 at 5% specimen elongation (magnification factor = 1).

away from the column web, as shown in Figure 3. These plates thus act both as continuity and doubler plates, and in this detail it is the intent that two doubler plates would always be used. This detail, first investigated by Bertero, Krawinkler, and Popov (1973), provides an economical alternative to connections that require two-sided doubler

plates plus four continuity plates. A parametric finite element study by Ye and others (2000) showed that the optimal location of the doubler plates so as to minimize the peak strains in the girder flange near the CJP weld is to place the doubler plates at a distance of  $\frac{1}{3}$  to  $\frac{2}{3}$  of the girder half flange width from the column web.



a)



b)

Fig. 7. Comparison of strain in the web vs. load for candidate pull-plate specimens: a) at a distance  $(5k+N)/2$  from the column centerline; b) at the column centerline.

Note that in later work as part of this project (Lee and others, 2002), it was determined with the steel fabricator that a better detail for the fillet-welded doubler plates of Specimens 1 and 2 (Figure 1) involves not beveling the doubler plate, as in those specimens. The standard, squared off doubler plate is cut to a width just under  $d - 2t_f$  of the column, is dropped into place, and is then fillet-welded to the column flange along its two sides. The gap opening would be typically less than that required to ensure prequalification of the fillet weld. However, it is not possible to weld across the top and bottom of the doubler plate in this configuration, although this is acceptable for typical connection behavior (Lee and others, 2002). This unbeveled, fillet-welded doubler plate detail is tested further in the cyclic cruciform girder-to-column joint experiments of Lee and others (2002).

The test specimens were designed to help determine if fillet welds or CJP welds are needed to adequately connect the continuity plates to the column flanges. The majority of the past research (e.g., Popov and others, 1986; Engelhardt and others, 1997; Engelhardt, 1999) in this area has recommended that complete-joint-penetration groove welds should be used. However, no tests have been done for the sole purpose of determining if fillet welds are adequate.

Yee and others (1998) performed finite element analyses that suggested that fillet welds would be sufficient for the continuity plate welds. The pull-plate experiments further contribute to this past research.

The column webs from the three proposed column sections ranged from 0.645 in. to 0.745 in. In comparison, the cruciform tests by Sherbourne and Jensen (1957) consisted of columns with web thicknesses ranging between 0.288 in. and 0.580 in., and Graham and others (1960) tested 11 pull-plate tests with web thicknesses in a similar range, 0.294 in. to 0.510 in. The web thicknesses tested in this research program represent realistic column sizes used in current practice. The column flange thicknesses, in turn, were in the range of the larger specimens tested by Graham and others (1960).

The CJP welds joining the pull plates to the column sections were made using the self-shielded FCAW process and E70T-6 filler metal. The E70T-6 wire had a diameter of 0.068 in. The filler metal used for the pull-plate specimens had a measured ultimate tensile strength of 77 ksi, and CVN values of 63.7 ft-lb at 70 °F and 19.0 ft-lb at 0 °F. Figure 4 shows the detail of the girder tension flange-to-column flange connection, including the weld type and access hole dimensions. Continuity plates and web doubler plates were

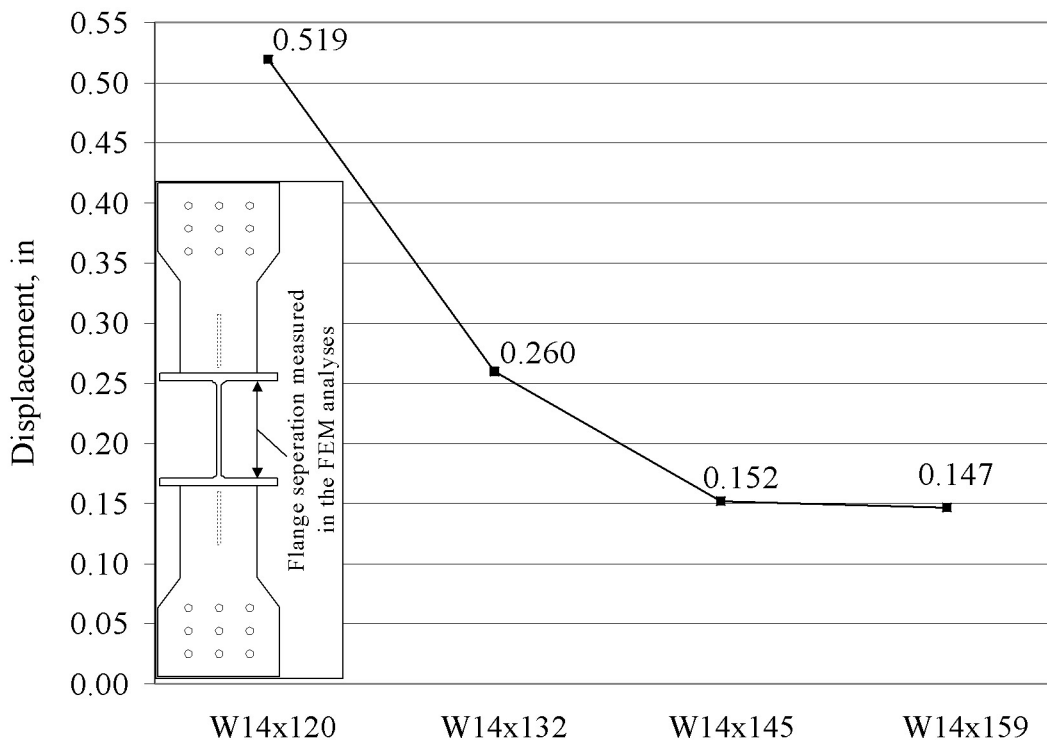


Fig. 8. Comparison of flange separation along outboard flange edge vs. column size for candidate pull-plate specimens.

**Table 2. Material Properties and Measured Dimensions of Pull-Plate Specimens  
(all units are kips and inches)**

	W14×132 (flange/web)	W14×145 (flange/web)	W14×159 (flange/web)	Pull-plate	HCP*	FCP*	DP*	DP Box*
<b>Coupon Yield (0.2% offset)</b>	49.2/54.4	58.2/59.4	51.1/ 55.2	48.2	50.0	46.0	56.2	46.5
<b>Mill Yield</b>	53.0	57.0	53.5	51.2	61.3	51.2	57.0	51.2
<b>Coupon Tensile</b>	69.4/70.3	74.1/75.1	71.5/71.8	72.5	72.2	72.5	73.8	72.5
<b>Mill Tensile</b>	70.5	73.5	72	72.1	80.4	72.1	71.0	72.1
$t_{cw}$	0.657	0.646	0.745	-	-	-	-	-
$t_{cf}$	0.998	1.073	1.187	-	-	-	-	-
$b_{cf}$	14.73	15.50	15.57	-	-	-	-	-
$k$	2.000	2.000	2.250	-	-	-	-	-

\* HCP = half-thickness continuity plate, FCP = full-thickness continuity plates, DP = doubler plate, DP Box = doubler plate box detail

fillet-welded using the 100 percent carbon dioxide gas-shielded FCAW process and E70T-1 filler metal with a 0.0625-in. diameter. For Specimen 6, CJP welds were used to join the continuity plate to the column flanges, and for Specimen 9, CJP welds were used to join the web doubler plate to the column flanges. These CJP welds were also made with the gas-shielded FCAW process and E70T-1 filler metal. The clips for the continuity plates were all ¾ in. on each side. As seen in Figure 4, a restrictor plate, representing a portion of the girder web, was tack welded to the girder flange and column flange before making the CJP weld for two reasons. The main reason was to simulate a bottom girder flange-to-column flange weld, in which the welder must stop and start the weld passes around the column web. A secondary reason for the restrictor plate was to keep the pull-plate at a 90° angle to the column flange. The column tack weld was removed before testing.

All plate material of the same thickness and columns with the same sizes were produced from the same heat. Table 2 presents a comparison of the coupon test results and the mill reports, as well as key measured dimensions of the actual cross sections tested. The columns were made from A992 steel, and the girders from A572 Gr. 50 plate. The reported coupon yield strength was defined by the 0.2 percent offset. All values given in Table 1 are averaged values from multiple coupons. Two coupons were taken from each flange and the web of each column section, and three coupons were taken from each plate. Rockwell hardness

values (B-scale) were also measured throughout the column cross sections. Along the column  $k$ -lines, the hardness values were shown to range from 78 to 90 for the W14×132, from 86 to 96 for the W14×145, and from 75 to 81 for the W14×159. Measured notch toughness in the  $k$ -line region for the three specimens ranged from 100 to 200 ft-lbs at 70 °F for all column sections. Prochnow and others (2000) provide further details of the ancillary testing for the pull-plate specimens, including documentation of the stress-strain parameters of the coupon tests, details of the CVN values and hardness values of the base metal, and transverse and longitudinal macrosections of typical regions of the E70T-6 CJP welds.

Testing of the pull-plate specimens followed the SAC protocol (SAC, 1997), where it was applicable. Since, the SAC protocol does not specify a strain rate for monotonic tensile tests, a high strain rate of 0.004 sec<sup>-1</sup> was used, which approximates the strain rate from seismic loading at about a 2 second period. The high strain rate increases the yield strength of the materials and increases the probability for brittle fracture, thereby testing the specimens under more severe conditions. There were three basic instrumentation plans, one for each of the three categories of specimens. All nine specimens had high-elongation strain gages on the pull-plates and LVDTs that measured the overall specimen elongation and the separation of the column flange tips. The data acquisition system collected 56 chan-

nels of data at 100 Hz. Prochnow and others (2000) provide further details of the testing procedure.

### ESTABLISHMENT OF FAILURE CRITERIA FOR LIMIT STATES

Before testing began, connection failure criteria were developed for the LWY and LFB limit states. The primary indicator of failure was whether the weld fractured prematurely. Brittle fracture was potentially still a possibility, because the fracture toughness of the E70T-6 weld metal was only somewhat better than the E70T-4 weld metal that was used in the pre-Northridge connections (FEMA, 2000c). If brittle fracture occurred in some cases but not in others, the influence of column stiffener details on the occurrence of brittle fracture could be investigated. However, there may be other undesirable behavior besides premature fracture, such as excessive deformation. In these experiments, none of the welds fractured prior to the pull plate fracturing, so secondary failure criteria were established based on excessive deformation to identify problematic limit states.

The criteria were established based on the results from finite element analyses conducted as part of this research (Ye and others, 2000), AISC provisions for LWY and LFB, and previous research [e.g., Sherbourne and Jensen (1957) and Graham and others (1960)]. For each specimen, the column section was examined for failure at non-seismic and seismic girder demand load levels,  $R_u$ , calculated as per Equations 8 and 9, respectively. Using the measured yield strength and girder flange (i.e., pull-plate) dimensions, the

non-seismic and seismic girder flange demands were approximately 360 and 435 kips, respectively. These were below nominal values because the coupon tests (Table 2) showed the 0.2 percent offset yield strength to be 48.2 ksi. The corresponding nominal values of 375 kips and 450 kips will be used for comparison to all results, because these represent values corresponding to design practice. In particular, for investigating the specimen behavior relative to the failure modes and yield mechanisms in this work, the pull-plate load of 450 kips (which corresponds to approximately 1.5 percent specimen elongation) will be used as the primary target for demand.

For each limit state, a two-part failure criterion was developed. The connection was classified as failing by LWY if at 450 kips the strain in the column  $k$ -line directly under the pull-plate was greater than 3.0 percent, or the strain in the column  $k$ -line was greater than the yield strain for the entire  $5k+N$  area. The connection was defined as failing by LFB if at 450 kips the separation of the two column flange tips on the same side of the web and located at the column centerline (as defined in Figure 7) was greater than  $\frac{1}{4}$  in. The LFB failure criterion was based on the permissible variations in cross section sizes given in ASTM (1998), which specifies that the flanges of a W-shape may be up to  $\frac{1}{4}$  in. out-of-square. Presumably, this amount of flange distortion is tolerable, such that the column is deemed to still have sufficient resistance to flange local buckling. Therefore, it was assumed that it would also be acceptable to have this much distortion caused by deforming of the girder flanges. The probability of an initially dis-

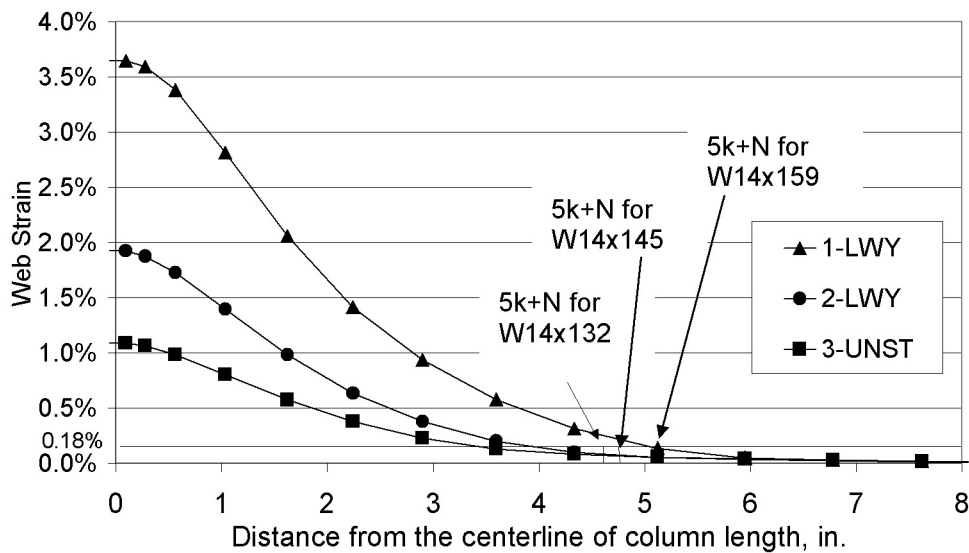


Fig. 9. Strain distribution from the finite element analyses along the column  $k$ -line at 450 kips.

torted flange combining with additional deformation due to the girder was deemed to be insignificant. The continuity plates, in turn, were characterized as failed if the entire full-width region of the continuity plates was above the yield strain.

Justification for the LWY failure criteria can be seen in Figures 6 and 9. Figure 6 exhibits the integral relation between the LWY and LFB failure modes in a typical unstiffened column. High strains in the column web directly opposite the girder flange contribute to LFB. Thus, in this research it was deemed important to track the strain along the column  $k$ -line throughout the  $5k+N$  region. Figure 9 shows finite element results similar to those seen in Figure 7, with the exception that mill report values are used for the yield and tensile strengths (as reported in Table 2). Using a similar failure criterion of Graham and others (1960), which based LWY failure on yielding (i.e., achieving a strain of 0.18 percent as shown in Figure 9) of the  $5k+N$  region of the column  $k$ -line, the W14×132 specimen would fail by LWY. Figure 9 shows that the strain in the W14×132 (1-LWY)  $k$ -line is greater than yield for the entire  $5k+N$  region, while the W14×145 (2-LWY) and W14×159 (3-UNST) are not. Therefore, if it is assumed that the W14×132 (1-LWY) fails and the W14×145 (2-LWY) does not, this establishes a second failure guideline used in this work relating to a strain greater than 3 percent directly below the pull-plate.

## EXPERIMENTAL RESULTS AND CORROBORATION WITH ANALYSIS

Table 3 is a summary of the pertinent results of the tests, including loads and specimen elongations when the specimen failed and when the different failure criteria were exceeded. Nominal strengths are computed using nominal material properties and the nominal section dimensions given in Table 1. Actual design strengths are calculated using the measured dimensions and material strengths given in Table 2. A discussion of results specific to the primary limit states follows.

### Local Web Yielding

Figure 10 shows the experimental strain distribution in the  $k$ -line of the column web for all seven specimens that were gaged to evaluate LWY. As shown in the figure, none of the specimens had strain levels exceeding 3 percent directly under the pull-plate at a load level of 450 kips, and only the unstiffened W14×145 specimen (2-LWY) had strain values greater than yield for the entire  $5k+N$  region. The W14×145 exhibits these higher strains relative to the W14×132 because measurements showed that the specific W14×145 section used in the test actually had a thinner web than the specific W14×132 section (see Table 2). There is no tolerance on web thickness in ASTM A6; the tolerance is only on the weight per foot (ASTM, 1998). The strain distribution also shows a much steeper gradient for the W14×132 (1-LWY) than the other two unstiffened sections. This gra-

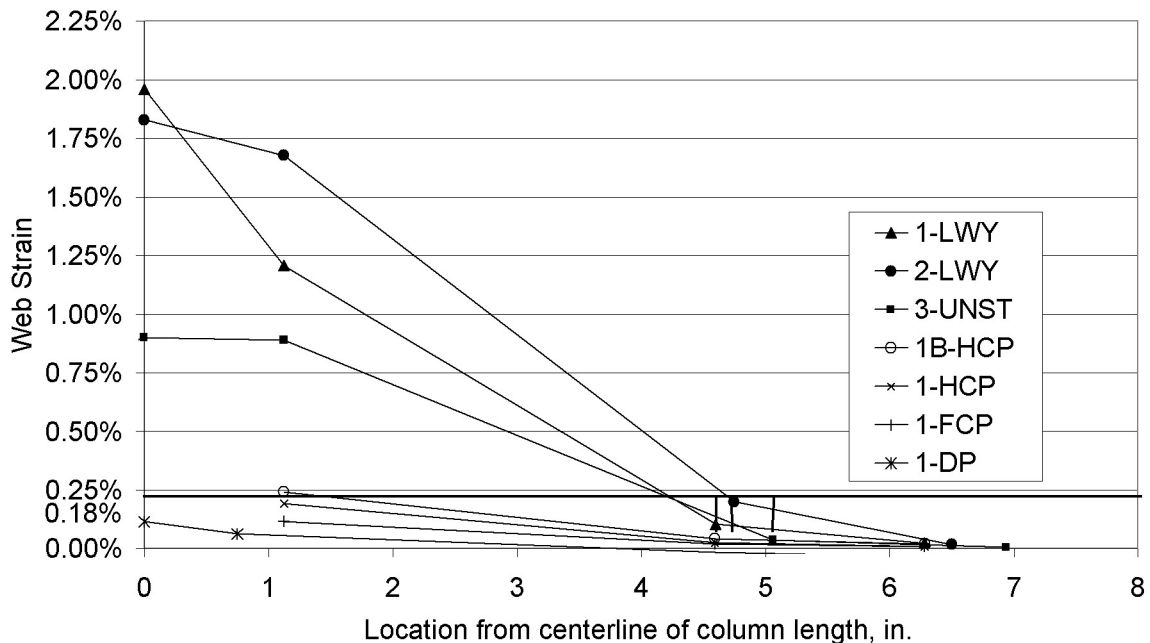


Fig. 10. Strain distribution from the experiments along the column  $k$ -line at 450 kips.

**Table 3. Experimental Test Results and Nominal and Actual Design Strengths of Pull-Plate Specimens**

	1-LWY	1-LFB	2-LWY	2-LFB	3-UNST	1-HCP	1B-HCP	1-FCP	1-DP
Ultimate Load / Specimen Elongation	523 k 4.7%	519 k 4.2%	519 k 3.8%	520 k 3.1%	520 k 3.5%	526 k 3.1%	548 k 4.3%	551 k 5.5%	527 k 2.6%
Load /Specimen Elongation at LWY YM 1*	471 k 2.2%	---	483 k 1.6%	---	514 k 3.2%	---	---	---	---
Load /Specimen Elongation at LWY YM 2**	500 k 3.3%	---	437 k 1.4%	---	496 k 2.7%	---	---	---	---
Nominal $\phi R_n$ for LWY Equation (1)	296 k		323 k		377 k				
Actual $\phi R_n$ for LWY Equation (1) <sup>#</sup>	384 k		413 k		493 k				
Load /Specimen Elongation at LFB YM <sup>†</sup>	412 k 1.1%	410 k 1.2%	463 k 1.9%	---	490 k 2.5%	---	---	---	---
Nominal $\phi R_n$ for LFB Equation (3)	298 k		334 k		398 k				
Actual $\phi R_n$ for LFB Equation (3) <sup>#</sup>	276 k		377 k		405 k				
Load /Specimen Elongation at Continuity Plate YM <sup>††</sup>	---	---	---	---	---	---	---	---	---
Load at 0.6% Specimen Elongation	379 k	382 k	381 k	276 k	274 k	365 k	383 k	387 k	399 k
Load at 1.5% Specimen Elongation	437 k	426 k	443 k	435 k	433 k	435 k	459 k	454 k	479 k

\* LWY YM 1 = local web yielding yield mechanism 1 = strain at the column length centerline in the *k*-line is above 3%

\*\* LWY YM 2 = local web yielding yield mechanism 2 = strain in the entire  $5k+N$  region of the *k*-line is above the yield strain

† LFB YM = local flange bending yield mechanism = flange tip separation is over 1/4 in.

†† CP YM = continuity plate yield mechanism = strain in the full-width region of the continuity plate is above the yield strain

# Actual  $\phi R_n$  values use measured specimen dimensions and coupon yield strength results as reported in Prochnow and others (2000)

**Table 4. Test-to-Predicted Ratios for Local Web Yielding Equations**

		1-LWY	2-LWY	3-UNST	Mean	Standard Deviation
Yield Mechanism Load, kips		500	437	496	-	-
Predicted Load, kips (Nominal)	Current LWY Eq (1)	296	323	377	-	-
	Quadratic Eq (10)	357	384	435	-	-
Test-to-Predicted Ratio (Nominal)	Current LWY Eq (1)	1.69	1.35	1.32	1.45	0.21
	Quadratic Eq (10)	1.40	1.14	1.14	1.23	0.15
Predicted Load, kips (Measured)	Current LWY Eq (1)	384	413	493	-	-
	Quadratic Eq (10)	430	462	512	-	-
Test-to-Predicted Ratio (Measured)	Current LWY Eq (1)	1.30	1.06	1.01	1.12	0.16
	Quadratic Eq (10)	1.16	0.95	0.97	1.03	0.12

dent is likely due to its thinner column flange. The thicker column flanges of the W14×145 and W14×159 act to distribute the load more evenly into the column web.

Figure 11 shows the deformation of Specimen 1-LWY at the end of the test, along with the approximate yielded zone. As seen in Figures 10 and 11, the W14×132 was close to breaching the LWY limit state at a load of 450 kips, and had breached the limit state at the time of failure at a load of 523 kips.

Equation 1 for LWY assumes a constant distribution of stress equal to the column web yield strength across the  $k$ -line for a distance  $5k+N$ . Figure 12 shows both the experimental and finite element method (FEM) stress distributions in the column web in the direction of loading of Specimens 1-LWY, 2-LWY, and 3-UNST. The stress distributions shown are at the load levels at which the entire  $5k+N$  region was above the yield strain of each column section (see Table 3). The experimental stress distributions were calculated by using the strain gage data along the  $k$ -line and the stress-strain behavior of the coupon results for the column webs [see Prochnow and others (2000) for details of this calculation]. The rectangular stress block inherent in Equation 1 for LWY only approximates the actual nonlinear stress distribution predicted both in the experiments and nonlinear

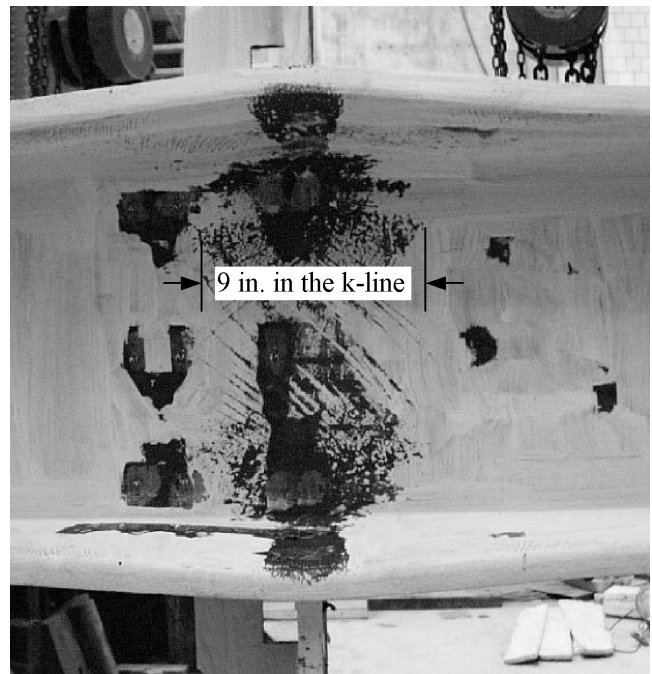


*Fig. 11. Deformation of specimen 1-LWY after the experiment.*

**Table 5. Comparison of Local Flange Bending Failure Loads**

Specimen	Column Shape	LFB Failure or Yield Mechanism Load, kips	Load Predicted by Equation (3), kips (Nominal)	Load Predicted by Equation (11), kips (Nominal)	Load Predicted by Equation (3), kips (Measured)	Load Predicted by Equation (11), kips (Measured)	Test-to-Predicted Ratio with Equation (3) (Nominal)	Test-to-Predicted Ratio with Equation (11) (Nominal)	Test-to-Predicted Ratio with Equation (3) (Measured)	Test-to-Predicted Ratio with Equation (11) (Measured)
1-LWY	W14x132	412	332	353	306	328	1.24	1.17	1.35	1.26
2-LWY	W14x145	463	371	362	419	442	1.25	1.28	1.11	1.05
3-UNST	W14x159	490	443	458	450	465	1.11	1.07	1.09	1.05
1-LFB <sup>#</sup>	W14x132	410	332	353	306	328	1.23	1.16	1.05	1.25
2-LFB <sup>#</sup>	W14x145	Never reached ¼ in. displ.	371	362	419	442	N.A.	N.A.	N.A.	N.A.
Mean							1.21	1.17	1.22	1.15
Standard Deviation							0.068	0.086	0.14	0.12

<sup>#</sup> Two ½ in. thick doubler plates added to column web

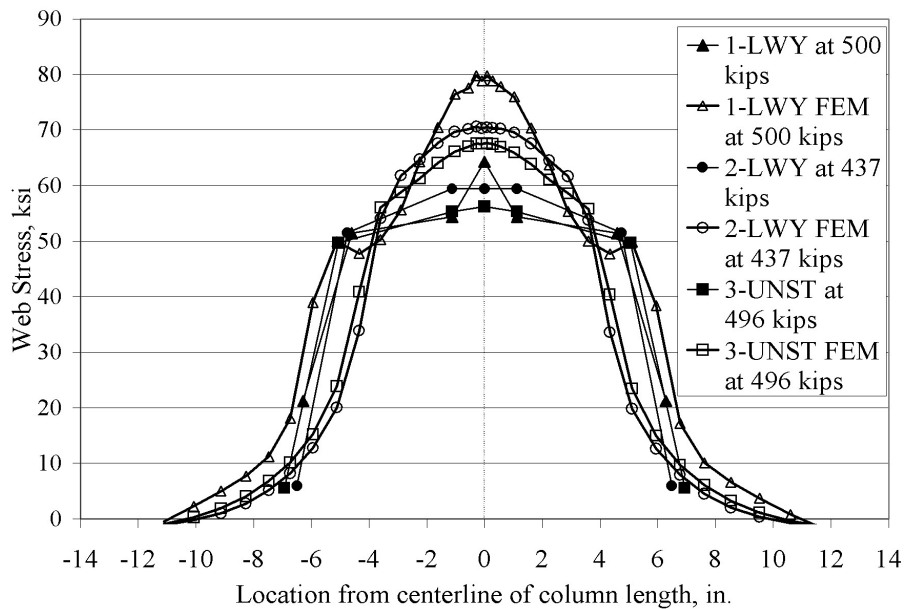


Fig. 12. Stress distributions along the column k-line.

analyses. To investigate the implications of this discrepancy, a quadratic curve was thus fit to the data for Specimens 1-LWY, 2-LWY, and 3-UNST at the respective load levels specified for yield mechanism 2 in Table 3. Integrating this stress along the distance  $5k+N$  yields a nominal strength for the local web yielding limit state:

$$R_n = \left(-0.023x^3 + 0.0007x^2 + 2.9x\right)t_{cw}F_{yc} \quad (10)$$

where  $x = (5k + N)/2$

Table 4 reports the predicted strength for LWY (using both nominal and measured properties as listed in Tables 1 and 2, respectively, without a  $\phi$  factor), according to Equations 1 and 10. Table 4 also reports the load at which LWY yield mechanism #2 was reached (as per Table 3). As may be seen in the table, the test-to-predicted ratio is consistently closer to 1.0 with the proposed design equation, and the standard deviations are smaller. However, it should be emphasized that the simpler equation currently in AISC (1999a), Equation 1, was compared both to the pull plate results in this research and to past work by Graham and others (1960) and in Prochnow and others (2000) and was found to be both reasonable and conservative for the non-seismic loading exhibited in these pull plate tests.

### Local Flange Bending

Figure 13 shows the separation of the flanges near the tips of the flanges along the column length for all nine speci-

mens. The W14×132 unstiffened and the W14×132 with doubler plates on the web (1-LFB) both failed this LFB criterion. By comparing the specimens without continuity plates but with web-doubler plates (1-LFB and 2-LFB) to those with no stiffeners at all (1-LWY and 2-LWY), it can be seen that a significant portion of the flange separation is due to web deformation, as confirmed by the finite element results of Figure 6 and the photograph in Figure 11. In the case of the W14×145 (2-LWY and 2-LFB), which has a stiffer flange and, as it turns out, a thinner web, half of the flange separation is due to web deformation.

The derivation of Equation 3 is based on the research of Graham and others (1960). Failure of their pull plate specimens was determined based upon fracturing. This is an unreliable failure mechanism for comparison with LFB predictions because it is based upon the toughness of the weld and base metal; the weld metal in particular was likely to be less tough than those used in the current pull plate tests. Prochnow and others (2000) thus show that the scatter in the test-to-predicted ratio of both the results of Graham and others (1960) and in the current work is significant. Thus, a new nominal strength equation for local flange bending has been derived in this work based upon a procedure similar to that used by Graham and others (1960), in which a plastic yield mechanism in the flange is assumed. Prochnow and others (2000) conducted a substantial parametric study of the range of yield mechanism parameters exhibited in typical girder-to-column connections, and thus simplified the proposed new local flange bending nominal

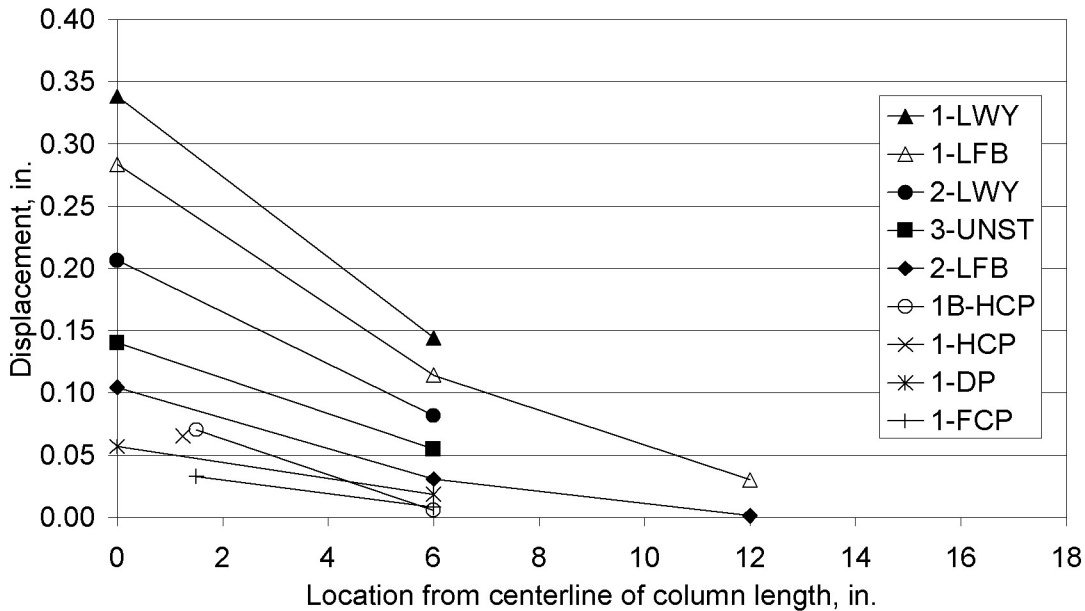


Fig. 13. Column flange separation from the experiments along the outboard flange edge column length at 450 kips.

strength equation to [see Prochnow and others (2000) for details of this derivation]:

$$R_n = (0.8 + 5.9t_{cf}^2) F_{yc} \quad (11)$$

Table 5 exhibits the predicted (using both nominal and measured properties as listed in Tables 1 and 2, respectively, without a  $\phi$  factor) and experimental strengths using the LFB yield mechanism reported in Table 3 and Equations 3 and 11. The test-to-predicted ratio of Equation 11 is consistently closer to 1.0 than Equation 3, and the standard deviations are similar. Prochnow and others (2000) show even more dramatic results when comparing to the test results of Graham and others (1960). However, it should be emphasized that Equation 3 was compared both to the pull plate results in this research and to past work by Graham and others (1960), and Equation 3 was found to be both reasonable and conservative for the non-seismic loading exhibited in these pull plate tests.

### Continuity and Doubler Plate Limit States

The results of the stiffened specimens (1-HCP, 1B-HCP, and 1-FCP) showed that, at least for monotonically loaded connections, a half-thickness continuity plate was adequate to avoid web yielding and flange bending. Figures 10 and 12 show a significant difference between the unstiffened and stiffened specimens. In particular, the specimens with fillet-welded half-thickness continuity plates (1-HCP and 1B-HCP) are well below the LWY and LFB failure criteria.

The failure criterion for the continuity plates was complete yielding across the full-width section of the plates at 450 kips. The full-width section of the continuity plates was

defined as the area just outside of the 3/4-in. clips. Figure 14 shows a comparison of the results of the strain distribution in the continuity plates of the 1-HCP and 1-FCP specimens. Neither of the specimens fully yielded across the width of the continuity plates, and therefore both were still capable of resisting load and had not failed. The half-thickness continuity plate fillet welds also did not fracture, thus validating the integrity of this detail. The CJP welds of the full-thickness continuity plates did not cause any problems during fabrication or testing.

Specimen 1-DP, the box detail, also performed well. Strains in the doubler plate and web did not exceed yield for the entire  $5k+N$  region, and neither the LWY nor the LFB limit states were breached. However, the doubler plates used in Specimen 1-DP were rather thick, based on the observation of Bertero and others (1973) that the doubler plates are less effective when they are moved away from the web. Equations 1 and 3 predict that two 3/32-in. doubler plates would be required to mitigate the LWY and LFB limit states, respectively using Equation 8 to compute girder flange demand. However, further research is required to determine an appropriate sizing procedure for the box detail. Note also that the backing bars used for the CJP welds of the doubler plates were not removed (and would not normally be removed for this detail), and the welds performed well in this test.

### CONCLUSIONS

This paper has given the background of the local web yielding and local flange bending limit states and the conclusions of previous researchers regarding the behavior of continuity plates and the welds attaching them to columns. It has also summarized the results of nine pull-plate tests and corresponding finite-element analyses studying column-stiffening details. The preliminary conclusions from these tests are focused on monotonic loading applications and will be synthesized with future cyclic loading experiments, with implications for seismic design, in Lee and others (2002) and other ongoing research. Conclusions of this paper, as related to non-seismic design, include:

- The AISC non-seismic design provisions for local web yielding and local flange bending are reasonable and slightly conservative in calculating the need for column stiffening. However, new design equations are also proposed in this research for the limit states of local flange bending and local web yielding in connections consisting of wide-flange girders framing into wide-flange columns with fully-restrained connections. When compared to experiments both from this research and past work, both equations provide superior test-to-predicted ratios as compared to current provisions. Broadening the range of experimental tests to include a wider range of

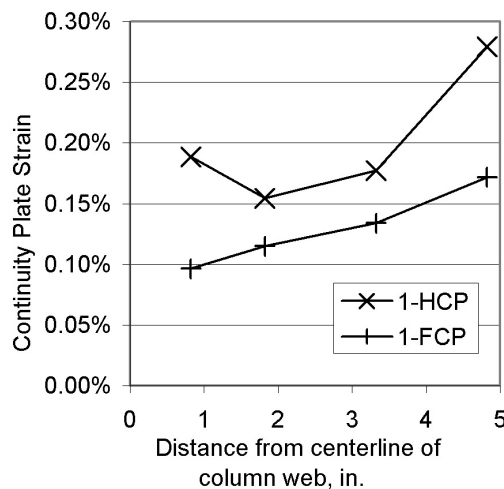


Fig. 14. Continuity plate stress distribution along full-width of plate of 450 kips.

section sizes would strengthen the assessment of these new equations.

- None of the E70T-6 CJP welds fractured despite plastic deformation, even when the flange tip separation was over ¼ in, indicating that column stiffener details may have little influence on the potential for brittle weld fracture provided the weld is specified with minimum CVN requirements and backing bars are removed.
- The use of half-thickness continuity plates fillet-welded to both the column web and flanges is sufficient for non-seismic design in comparison to the traditional full-thickness continuity plates with CJP welds.
- The new doubler plate details, i.e., the box detail and beveled doubler plates fillet-welded to the column flanges, both of which avoid welding to the column *k*-line, performed satisfactorily under monotonic loading and provided sufficient stiffness to avoid the local web yielding and local flange bending limit states for non-seismic design.

#### ACKNOWLEDGMENTS

Funding for this research was provided by the American Institute of Steel Construction and the University of Minnesota. In-kind funding and materials were provided by LeJeune Steel Company, Minneapolis, Minnesota; Danny's Construction, Minneapolis, Minnesota; Braun Intertec, Minneapolis, Minnesota; Nucor-Yamato Steel Company, Blytheville, Arkansas; and Lincoln Electric Company, Cleveland, Ohio; and Edison Welding Institute, Cleveland, Ohio. Supercomputing resources were provided by the Minnesota Supercomputing Institute. The authors gratefully acknowledge this support. The authors would also like to thank Messrs. L.A. Kloiber, LeJeune Steel Company, P.M. Bergson, University of Minnesota, and the members of the external advisory group on this project for their valuable assistance with this research.

#### REFERENCES

- American Institute of Steel Construction (AISC) (1937), *A Manual for Architects, Engineers and Fabricators of Buildings and Other Steel Structures*, 3rd Edition, AISC, New York, New York.
- AISC (1989), *Manual of Steel Construction—Allowable Stress Design*, 9th Edition, AISC, Chicago, Illinois.
- AISC (1992), *Seismic Provisions for Structural Steel Buildings*, AISC, Chicago, Illinois.
- AISC (1993), *Load and Resistance Factor Design Specification for Structural Steel Buildings*, AISC, Chicago, Illinois.
- AISC (1995), *Manual of Steel Construction—Load and Resistance Factor Design*, 2nd Edition, AISC, Chicago, Illinois.
- AISC (1997a), *Seismic Provisions for Structural Steel Buildings*, AISC, Chicago, Illinois.
- AISC (1997b), "AISC Advisory on Mechanical Properties Near the Fillet of Wide Flange Shapes and Interim Recommendations, January 10, 1997," AISC, Chicago, Illinois.
- AISC (1999a), *Load and Resistance Factor Design Specification for Structural Steel Buildings*, AISC, Chicago, Illinois.
- AISC (1999b), *Stiffening of Wide-Flange Columns at Moment Connections: Wind and Seismic Applications*, Steel Design Guide Series 13, AISC, Chicago, Illinois.
- AISC (2000), *Seismic Provisions for Structural Steel Buildings (1997)—Supplement No. 2*, AISC, Chicago, Illinois.
- AISC (2001), "AISC Advisory on Changes to T, k, and k1 Dimensions for W-Shapes, February 14, 2001," AISC, Chicago, Illinois.
- AISC (2002), *Seismic Provisions for Structural Steel Buildings*, AISC, Chicago, Illinois.
- American Society of Testing and Materials (ASTM) (1998), *ASTM A6/A6M: Standard Specification for General Requirements for Rolled Structural Steel Bars, Plates, Shapes, and Sheet Piling*, ASTM, Conshohocken, Pennsylvania.
- Bertero, V.V., Krawinkler, H., and Popov, E.P. (1973), "Further Studies on Seismic Behavior of Steel Beam-Column Subassemblages," Report No. EERC-73/27, Earthquake Engineering Research Center, University of California, Berkeley, California.
- Bjorhovde, R., Golland, L.J., and Benac, D.J. (1999), "Tests of Full-Scale Beam-to-Column Connections," *Internal Report*, Southwest Research Institute, San Antonio, Texas.
- Bruneau, M., Uang, C.-M., and Whittaker, A. (1998), *Ductile Design of Steel Structures*, McGraw-Hill, New York, New York.
- Dexter, R.J., Hajjar, J.F., Cotton, S.C., Prochnow, S.D., and Ye, Y. (1999), "Reassessment of Design Criteria and New Alternatives for Column Transverse Stiffeners (Continuity Plates) and Web Doubler Plates: Interim Report," *Report No. ST-99-3*, Department of Civil Engineering, University of Minnesota, Minneapolis, Minnesota.
- Dexter, R.J. and Melendrez, M.I. (2000), "Through-Thickness Properties of Column Flanges in Welded Moment Connections," *Journal of Structural Engineering*, ASCE, Vol. 126, No. 1, pp. 24-31.

- El-Tawil, S., Vidarsson, E., Mikesell, T., and Kunnath, S. (1999), "Inelastic Behavior and Design of Steel Panel Zones," *Journal of Structural Engineering*, ASCE, Vol. 125, No. 2, pp. 183-193.
- Engelhardt, M.D., Shuey, B.D., and Sabol, T.A. (1997), "Testing of Repaired Steel Moment Connections," *Proceedings of the ASCE Structures Congress*, Kempner, L. and Brown, C. (eds.), April 13-16, 1997, pp. 408-412, Portland, Oregon.
- Engelhardt, M.D. (1999), "Design of Reduced Beam Section Moment Connections," Proceedings of the AISC North American Steel Construction Conference, Toronto, Ontario, May 19-21, 1999, AISC, Chicago, Illinois.
- Federal Emergency Management Agency (FEMA) (1995), "Interim Guidelines: Inspection, Evaluation, Repair, Upgrade and Design of Welded Moment Resisting Steel Structures," *Report No. FEMA-267*, Federal Emergency Management Agency, Washington, D.C.
- FEMA (1996), "Interim Guidelines: Advisory No. 1," Report No. FEMA-267A, Federal Emergency Management Agency, Washington, D.C.
- FEMA (1999), "Interim Guidelines: Advisory No. 2," *Report No. FEMA-267B*, Federal Emergency Management Agency, Washington, D.C.
- FEMA (2000a), "Recommended Seismic Design Criteria for New Steel Moment-Frame Buildings," *Report No. FEMA-350*, Federal Emergency Management Agency, Washington, D.C.
- FEMA (2000b), "State-of-the-Art Report on Base Metals and Fracture," *Report No. FEMA-355A*, Federal Emergency Management Agency, Washington, D.C.
- FEMA (2000c), "State-of-the-Art Report on Joining and Inspection," *Report No. FEMA-355B*, Federal Emergency Management Agency, Washington, D.C.
- FEMA (2000d), "State-of-the-Art Report on Connection Performance," *Report No. FEMA-355D*, Federal Emergency Management Agency, Washington, D.C.
- Graham, J.D., Sherbourne, A.N., Khabbaz, R.N., and Jensen, C.D. (1960), "Welded Interior Beam-to-Column Connections," Welding Research Council, *Bulletin No. 63*, pp. 1-28.
- Johnson, L.G. (1959a), "Tests on Welded Connections between I-Section Beams and Stanchions," *British Welding Journal*, Vol. 6, No. 1, pp. 38-46.
- Johnson, L.G. (1959b), "Further Tests on Welded Connections between I-Section Beams and Stanchions," *British Welding Journal*, Vol. 6, No. 1, pp. 367-373.
- Johnson, L.G. (1959c), "Compressive and Tensile Loading Tests on Joists with Web Stiffeners," *British Welding Journal*, Vol. 6, No. 1, pp. 411-420.
- Kaufmann, E.J., Xue, M., Lu, L.W., and Fisher, J.W. (1996), "Achieving Ductile Behavior of Moment Connections," *Modern Steel Construction*, AISC, January, pp. 30-39, Chicago, Illinois.
- Krawinkler, H., Bertero, V.V., and Popov, E.P. (1971), "Inelastic Behavior of Steel Beam-to-Column Subassemblies," *Report No. EERC-71/7*, Earthquake Engineering Research Center, University of California, Berkeley, California.
- Krawinkler, H. (1978), "Shear in Beam-Column Joints in Seismic Design of Steel Frames," *Engineering Journal*, AISC, Vol. 15, No. 3, pp. 82-91.
- Lee, D., Cotton, S.C., Dexter, R.J., Hajjar, J.F., Ye, Y., and Ojard, S.D. (2002), "Column Stiffener Detailing and Panel Zone Behavior of Steel Moment Frame Connections," *Report No. ST-01-3.2*, June, Department of Civil Engineering, University of Minnesota, Minneapolis, Minnesota.
- Parkes, E.W. (1952), "The Stress Distribution Near a Loading Point in a Uniform Flanged Beam," *Philosophical Transactions of the Royal Society*, Vol. 244A, pp. 417-467.
- Popov, E.P., Amin, N.R., Louie, J.J., and Stephen, R.M. (1986), "Cyclic Behavior of Large Beam-column Assemblies," *Engineering Journal*, AISC, Vol. 23, No. 1, pp. 9-23.
- Prochnow, S.D., Dexter, R.J., Hajjar, J.F., Ye, Y., and Cotton, S.C. (2000), "Local Flange Bending and Local Web Yielding Limit States in Steel Moment-Resisting Connections," *Report No. ST-00-4*, Department of Civil Engineering, University of Minnesota, Minneapolis, Minnesota.
- Ricles, J.M., Mao, L., Kaufmann, E.J., Lu, L., and Fisher, J.W. (2000), "Development and Evaluation of Improved Details for Ductile Welded Unreinforced Flange Connections," *Report No. SAC/BD-00/24*, SAC Joint Venture, Sacramento, California.
- Roeder, C.W. (1997), "An Evaluation of Cracking Observed in Steel Moment Frames," *Proceedings of the ASCE Structures Congress*, Kempner, L. and Brown, C. (eds.), Portland, Oregon, April 13-16, 1997, pp. 767-771, ASCE, New York, New York.
- SAC Joint Venture (SAC) (1997), "Protocol for Fabrication, Inspection, Testing, and Documentation of Beam-Column Connection Tests and Other Experimental Specimens," *Report No. SAC/BD-97/02*, SAC Joint Venture, Sacramento, California.
- Sherbourne, A.N., and Jensen, C.D. (1957), "Direct Welded Beam Column Connections," *Report No. 233.12*, Fritz Laboratory, Lehigh University, Bethlehem, Pennsylvania.

- Tide, R.H. (2000), "Evaluation of Steel Properties and Cracking in the 'k' -area of W Shapes," *Engineering Structures*, Vol. 22, pp. 128-124.
- Tremblay, R., Timler, P., Bruneau, M., and Filiatrault, A. (1995), "Performance of Steel Structures During the 1994 Northridge Earthquake," *Canadian Journal of Civil Engineering*, Vol. 22, pp. 338-360.
- Wood, R.H. (1955), "Yield Line Theory," *Research Paper No. 22*, Building Research Station.
- Webster, D. (2000), "Report on the Change in Model Material Properties Used for ABAQUS Finite Element Analysis," *Internal Report*, Department of Civil Engineering, University of Minnesota, Minneapolis, Minnesota.
- Xue, M., Kaufmann, E.J., Lu, L.W., and Fisher, J.W. (1996), "Achieving Ductile Behavior of Moment Connections, Part II," *Modern Steel Construction*, AISC, June, pp. 38-42, Chicago, Illinois.
- Ye, Y., Hajjar, J.F., Dexter, R.D., Prochnow, S.C., Cotton, S.C. (2000), "Nonlinear Analysis of Continuity Plate and Doubler Plate Details in Steel Moment Frame Connections," *Report No. ST-00-3*, Department of Civil Engineering, University of Minnesota, Minneapolis, Minnesota.
- Yee, R.K., Paterson, S.R., and Egan, G.R. (1998), "Engineering Evaluations of Column Continuity Plate Detail Design and Welding Issues in Welded Steel Moment Frame Connections," *Welding for Seismic Zones in New Zealand*, Aptech Engineering Services, Inc., Sunnyvale, California.